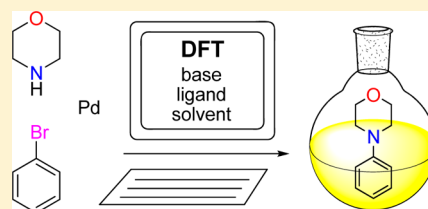


## Role of the Base in Buchwald–Hartwig Amination

Ylva Sunesson,<sup>†</sup> Elaine Limé,<sup>‡</sup> Sten O. Nilsson Lill,<sup>‡</sup> Rebecca E. Meadows,<sup>§</sup> and Per-Ola Norrby<sup>\*,†,‡</sup><sup>†</sup>Department of Chemistry and Molecular Biology, University of Gothenburg, Kemigården 4, SE-412 96 Göteborg, Sweden<sup>‡</sup>Pharmaceutical Development, Global Medicines Development, AstraZeneca, Pepparedsleden 1, SE-431 83 Mölndal, Sweden<sup>§</sup>Pharmaceutical Development, AstraZeneca, Silk Road Business Park, Macclesfield SK10 2NA, United Kingdom

## S Supporting Information

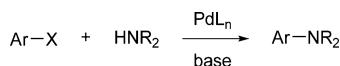
**ABSTRACT:** The Buchwald–Hartwig amination has been investigated theoretically and experimentally to examine the scope of possible bases under different reaction conditions. Nonpolar solvents resist the formation of new charges. Therefore, the base should be anionic to be able to deprotonate the neutral palladium–amine complex and/or expel the anionic leaving group (bromide). The calculated barrier for the organic base DBU was found to be prohibitively high. In polar solvent, dissociation of bromide becomes possible, but here the base will instead form a complex with palladium, creating an overly stable resting state. The conclusions for both solvent classes hold for both a hindered monodentate phosphine and the labile bidentate ligand BINAP. The computational studies were supported by experimental testing of a range of bases using BINAP in two different solvents, toluene and DMF.



## ■ INTRODUCTION

Aryl amines are ubiquitous in natural products and druglike substances. As a consequence, the development of metal-mediated protocols for their synthesis has been of immense importance in both industry and academia. A key example of this, the palladium-catalyzed Buchwald–Hartwig aryl amination (Scheme 1),<sup>1</sup> is now regarded as a vital tool in the organic chemist's synthesis toolbox.<sup>2</sup>

## Scheme 1. General Scheme for Buchwald–Hartwig Aryl Amination



Because of extensive experimental<sup>3–5</sup> and theoretical<sup>4–7</sup> investigations, we know much about the mechanism and special requirements of the Buchwald–Hartwig reaction.<sup>8</sup> A simplified catalytic cycle summarizing the more important findings is depicted in Figure 1. The precatalyst forms a Pd(0)–ligand complex that undergoes oxidative addition with the aryl electrophile, in common with most palladium-catalyzed coupling mechanisms. In the next step, the amine nucleophile is coordinated to the metal and deprotonated by the base. The catalytic cycle is closed by reductive elimination, yielding the final arylated amine product while regenerating the active catalyst.

Only certain ligands function well in this cycle. Among the most widely used are the Buchwald family of electron-rich monophosphine ligands.<sup>9</sup> Their mode of binding to the Pd center does in fact display some bidentate character through  $\pi$ -coordination from the second aryl ring, as has been shown both experimentally<sup>10</sup> and by crystallization of the intermediate

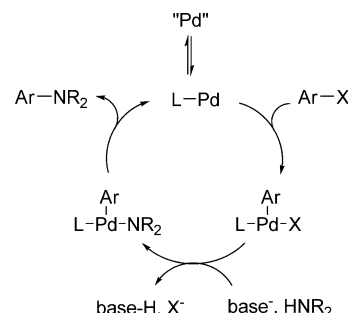


**Figure 1.** Simplified catalytic cycle for Buchwald–Hartwig aryl amination.

complexes.<sup>11</sup> In Pd(II) complexes with hindered monodentate or hemilabile ligands like the biaryl phosphines, the strong *trans* effect of the aryl group allows the formation of T-shaped complexes where the position *trans* to the aryl group is empty,<sup>12</sup> opening a facile entry path for the amine substrate. The hemilabile behavior can also be displayed with some bisphosphine ligands, such as BINAP, allowing this class of ligand to also result in effective catalysis of the reaction (*vide infra*).

The detailed order of the coordination and deprotonation steps is still unclear, with several complexes in rapid and not easily studied equilibrium.<sup>8</sup> It is obvious from relative  $\text{pK}_a$  values that the amine can be deprotonated by commonly used bases like alkoxides only if the amine has already been activated by coordination to the metal. However, it is not known whether the base always has to coordinate first, expelling the leaving

**Special Issue:** Mechanisms in Metal-Based Organic Chemistry

**Received:** August 6, 2014

**Published:** October 23, 2014

group X, or whether an external base can deprotonate the amine in a coordinatively saturated square planar palladium complex. The details of this part of the catalytic cycle may be important in determining which bases can be competent in the overall reaction.

Experimentally, it is necessary to distinguish between different types of amine nucleophiles. Anilines and other moderately acidic nitrogen functionalities like amides are easily arylated even when the base is relatively mild and/or unhindered (e.g., hydroxide and substituted phenolates).<sup>13</sup> On the other hand, dialkyl amines are more resistant to deprotonation and seem to require *tert*-butoxide or other alkoxide bases of similar basicity.<sup>1c</sup> As a corollary, dialkyl amine arylation requires more rigorous drying than the corresponding aniline arylation, because trace water will convert any strong base to relatively weak hydroxide, reducing the efficiency in the reaction of alkyl amines.

This work stems from a project in which Buchwald–Hartwig amination is performed in flow. Successful implementations have already been reported by others<sup>14,15</sup> for the relatively simple and water-tolerant case of aniline arylation. For the purpose of this study, we wish to focus on a pharmaceutically relevant reaction between an aryl bromide and a dialkyl amine. Under these circumstances, bases such as *t*-BuOK or *t*-BuONa in combination with an aryl bromide will lead to production of KBr or NaBr, respectively, each of which has a low solubility in solvents that are compatible with arylation of alkyl amines<sup>15</sup> and are therefore incompatible with most flow reactors. In this work, we were interested in investigating whether it is possible to use an alternative, neutral base that will avoid precipitation in a relevant solvent (i.e., a solvent that will not react with strong bases).

We investigated our chosen reaction both experimentally and computationally. To facilitate the theoretical study, we chose experimentally relevant, small model systems to avoid extensive conformational equilibrations (Figure 2). As a starting point,

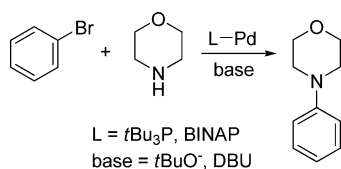


Figure 2. Model systems used in this study.

we selected the simplest possible electrophile, phenyl bromide, and a pharmaceutically relevant yet simple amine, morpholine. Of the experimentally competent ligands, the simplest is *t*-Bu<sub>3</sub>P, introduced into Buchwald–Hartwig amination by Nishiyama et al.<sup>16</sup> and shortly thereafter demonstrated to allow coupling at room temperature when Hartwig and co-workers used a 1:1 ratio of ligand to palladium.<sup>17</sup> The same model system was recently studied by McMullin et al., using similar computational methods.<sup>6</sup> Most of our computational studies have been performed with this small model system. On the basis of the results from the smaller system, we have also extended our study to include the BINAP ligand, as well as an alternative substrate, *N*-methylpiperazine. We have also challenged our predictions about reactivity under different conditions by experimental testing.

The most frequently used bases in the arylation of alkyl amines are *tert*-alkoxides; therefore, we chose the simplest representative of this class of base, *t*-BuO<sup>−</sup>, for our computa-

tional study.<sup>4</sup> Experimentally, both sodium and potassium salts work well. In the theoretical study, the counterion gives intractable problems with solvent coordination and conformational sampling.<sup>18</sup> Thus, we did not include the counterion in any of our calculations. We note that charge separation leads to high uncertainties in energies calculated with continuum solvation models and therefore avoid drawing conclusions from small calculated energy differences between complexes with different overall charges.

1,8-Diazabicyclo[5.4.0]undec-7-ene (DBU) has been demonstrated to function well in the arylation of anilines under microwave irradiation<sup>19</sup> and was therefore our primary candidate in the computational study. We were also interested in solvents with different polarities and how they would affect the preference for different mechanistic pathways with both types of bases. We therefore selected two solvents with ample experimental precedent, nonpolar toluene (simulated by continuum parameters for benzene) and polar aprotic DMF. Computationally, these were represented by continuum models.

DFT calculations were conducted at the B3LYP/LACVP\* level, with corrections for dispersion as specified in the computational details. Geometries were determined in the gas phase, with thermodynamic and solvation corrections calculated at the final converged geometries. Only final free energies are reported; all energy components used in the calculation of the final energies can be found as Supporting Information.

All free energies herein are based on the B3LYP-D3 results, but to test the method dependence, we have also recalculated the most important energies using M06/LACV3P\*. The relative energies of different points on the path, found in the Supporting Information, change by only 2–4 kJ mol<sup>−1</sup> when going from B3LYP-D3 to M06.

## RESULTS AND DISCUSSION

The Buchwald–Hartwig amination has been studied theoretically by McMullin et al.<sup>6</sup> Our methods differ slightly from theirs (we include a dispersion correction in the final free energies and use a smaller basis set), but for large parts of the reaction, our results agree closely. We will here summarize briefly our results for the parts of the mechanism in which our studies overlap, before going into the major focus of our study, the role of the base. The major common features of the free energy profile (FEP) are depicted in Figure 3.

The starting point in a catalytic cycle is arbitrary, but visual identification of selectivity-determining steps depends on comparing with steps on both sides.<sup>20</sup> It is therefore good practice to duplicate parts of the FEP to allow rapid visual identification of important reaction features.<sup>21</sup> We have elected here to include the reductive elimination transition state (RE TS) and the prereactive complex **5** twice in Figure 3. Thus, the first instance of **5** and RE includes the energies of all the reagents (PhBr, morpholine, and *t*-BuO<sup>−</sup>), whereas the second instance includes the energies of all products (*N*-phenylmorpholine, *t*-BuOH, and Br<sup>−</sup>). We have chosen to use the energy of the RE TS as a reference, allowing a simple determination of the overall barrier as the negative of the energy of the lowest preceding point on the FEP. The difference between the two occurrences of the RE TS corresponds to the overall calculated exergonicity of the catalytic cycle, 294 kJ mol<sup>−1</sup> in benzene with *tert*-butoxide as the base.

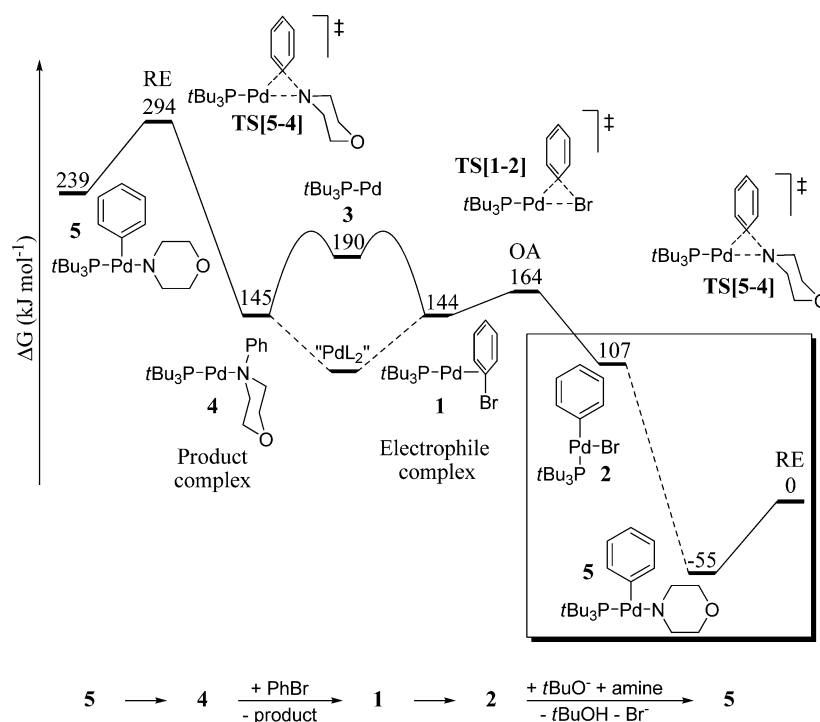


**Figure 3.** Free energy profile (FEP) of the catalytic cycle in benzene. Curved lines represent monotonous reactions without a potential energy barrier, that is, a diffusion-controlled free energy barrier of  $\sim 20 \text{ kJ mol}^{-1}$  to association.<sup>22</sup> Dotted lines show multistep reactions with expected low barriers, but potentially including low-energy intermediates. The boxed area includes multiple steps that we investigated further (*vide infra*).

Looking at the overall shape of the FEP in Figure 3, we see that we have two effectively irreversible steps (i.e., transition states that are higher than all subsequent points on the FEP<sup>20</sup>), the oxidative addition (OA) and the reductive elimination (RE). For each of these, the energy barrier is the difference between the TS energy and the energy of the lowest preceding point. We will discuss each of these steps in turn.

In here, we will first briefly summarize our findings for the oxidative addition and reductive elimination, where the results are similar to those of previous studies, whereupon we will report more extensively on the coordination and proton shift equilibria found in the Pd(II) part of the catalytic cycle (the boxed part of Figure 3).

**Oxidative Addition.** The oxidative addition is common to most palladium-catalyzed couplings and has been investigated in detail.<sup>8</sup> The starting point, a Pd(0) complex, can be generated in many different ways, but with hindered phosphines like *t*-Bu<sub>3</sub>P, it is now well established that the path goes through a Pd(0) complex with the aryl bromide and one ligand (1).<sup>22</sup> The transition state TS[1–2] for conversion of 1 to the oxidative addition product 2 is only  $20 \text{ kJ mol}^{-1}$  above 1 in benzene, in qualitative agreement with earlier studies.<sup>23</sup> Complex 1 can be obtained by association of aryl bromide to a monoligated Pd(0) complex (3)<sup>23</sup> or by associative displacement with other bis-ligated Pd(0) complexes.<sup>22</sup> In a recent study, McMullin et al. concluded that the associative displacement is the most likely option for aryl bromides,<sup>22</sup> and our current results are well aligned with this conclusion. The mono-phosphine–Pd complex 3 is  $>40 \text{ kJ mol}^{-1}$  higher in energy than either the reactant complex 1 or the product complex 4, and even  $26 \text{ kJ mol}^{-1}$  higher than the OA TS, making it unlikely that 3 is on the true reaction path. There are several other potential intermediates or off-cycle Pd(0) complexes, such as a bis-phosphine complex or Pd

complexes of other frequently employed species like dba.<sup>24</sup> The bis-phosphine complex has been shown to be substantially more stable than prereactive complex 1, leading to an effective increase in the activation barrier.<sup>23</sup> The barrier to oxidative addition would be the energy difference between TS[1–2] and the lowest energy of any kinetically accessible Pd(0) complex preceding the OA TS. However, in general, this step is not expected to be rate-limiting with a good leaving group like bromide, especially not when the ligands have been chosen to be strongly hindered, avoiding the formation of low-energy polyligated Pd(0) complexes.<sup>25</sup>

The immediate oxidative addition product, complex 2, is  $57 \text{ kJ mol}^{-1}$  lower in energy than the OA TS. Thus, the reverse reaction does not have a very high barrier. However, in this case, it can easily be seen that the OA TS is higher in energy than all subsequent points, making the step effectively irreversible,<sup>20</sup> as any intermediate will prefer a forward rather than a backward reaction.

**Reductive Elimination.** In close accordance with the study of McMullin et al.,<sup>6</sup> we find that the preferred reductive elimination occurs from the T-shaped complex 5, where again the position *trans* to the phenyl group is empty (Figure 3). Hoi et al. also investigated a transition state for a square planar complex with an additional bound amine and found it to be higher in free energy than the corresponding TS arising from a T-shaped complex.<sup>4</sup> In close agreement with the situation seen in the oxidative addition, the product complex (4) is substantially more stable than the separated components (3 + product), by  $\sim 45 \text{ kJ mol}^{-1}$ ; the product complex 4 has a stability very similar to that of the reactant complex 1. As discussed in connection with the oxidative addition, this is just one of many possible Pd(0) complexes, and not the most stable one.<sup>23</sup>

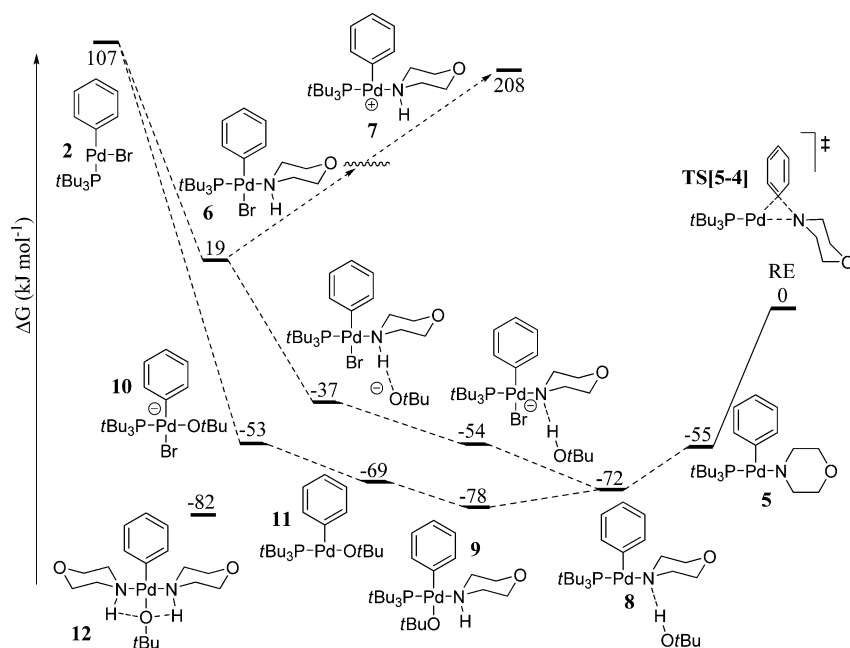


Figure 4. Pd(II) section of the reaction in benzene with  $t\text{-BuO}^-$  as the base.

The transition state for oxidative addition is  $164 \text{ kJ mol}^{-1}$  higher in energy than the transition state for reductive elimination when looking in the forward reaction direction. It should be noted that this energy difference is very sensitive to the exact experimental conditions. The intervening steps include the dissociation of bromide and the action of the base on the amine. Thus, an immediate effect of changing the base strength is that the relative energy of these two transition states will change. It should also be realized that all calculated energies refer to a standard state in which all species considered have a concentration of  $1 \text{ M}$ .<sup>26</sup> The reality is of course much different, and in nonpolar solvents in particular, the bromide concentration will be severely limited by solubility. If the bromide liberated from **2** precipitates out of solution, the bromide dissociation will, in effect, be irreversible, irrespective of the calculated energy.

Changing the solvent and base has an only minor effect on the relative energies of all steps in Figure 3 up to the oxidative addition but can have a very strong effect on subsequent steps. We will now look in detail at the effects in the boxed region of Figure 3, from OA to RE, and discuss different bases and solvents separately.

**Alkoxide Base in a Nonpolar Solvent.** The potential intermediates on the path from oxidative addition product **2** up to the reductive elimination, TS[5-4], are shown in Figure 4. The overall computational system is anionic; energies for intermediates shown as neutral also include the energy of the separated anion, *tert*-butoxide or bromide. We take as the starting point the T-shaped OA product, complex **2**, which has an open coordination site. Such complexes are configurationally labile, in particular when one ligand has a free electron pair that can be used to migrate to a neighboring open site (Figure 5).<sup>12</sup> Thus, as long as the T-shaped complexes are energetically accessible, *cis* and *trans* forms will equilibrate rapidly. We only show the most stable form of each complex in Figure 4. The two ligands with the strongest *trans* effects will have an electronic preference for a *cis* arrangement, but the steric cost for this arrangement can be high.<sup>27</sup> Among the remaining

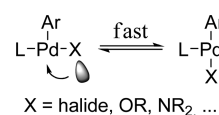


Figure 5. T-Shaped complexes are labile when one ligand has a free lone pair.<sup>12</sup>

ligands, the one with the weakest *trans* effect (or the empty coordination site) will have an electronic preference for a position *trans* to the aryl group.<sup>12</sup>

The amine or base can coordinate to the empty site of one of the *cis-trans* isomers of **2**. Association to an empty coordination site is generally calculated to be a monotonous downhill process and thus can be seen as a diffusion-controlled process with an effective free energy barrier of  $\sim 20 \text{ kJ mol}^{-1}$ .<sup>22</sup> Considering first the direct amine coordination, the resulting square planar complex **6** will be deprotonated and the bromide will be dissociated before reductive elimination, but the order of these steps is not *a priori* obvious. However, in the nonpolar solvent, it is clear that dissociation of bromide from a neutral Pd complex, leading to charge separation, is strongly disfavored. Formation of the separated ion pair (**7**) is endergonic by  $189 \text{ kJ mol}^{-1}$ . On the other hand, association of the base with a hydrogen bond from the coordinated amine is strongly favored, and the proton transfer occurs with a negligible barrier. The bromide is dissociated from the resulting anionic complex in an exergonic process, to yield neutral complex **8**, which retains a hydrogen bond to the protonated base,  $t\text{-BuOH}$ . Dissociation of  $t\text{-BuOH}$  leads to complex **5**, which undergoes reductive elimination as already discussed.

Complex **8** is a T-shaped complex with an open coordination site and is thus in equilibrium with several more stable species, leading to an increase in the effective barrier. The hydrogen-bonded  $t\text{-BuOH}$  can migrate to the open coordination site and will simultaneously transfer the proton back to the amide in a concerted process to yield complex **9**. The same complex could also be formed directly from **2** through association of the base to yield anionic complex **10**, dissociation of bromide to give T-



shaped complex **11**, and finally association of the amine to give **9**. Because all barriers are low, it does not matter by which paths the low-energy complexes are formed. As long as all transition states are significantly below that of TS[5–4], the kinetic profile of the reductive elimination will depend on only the nature of the lowest-energy preceding point, the resting state. At  $-78 \text{ kJ mol}^{-1}$ , complex **9** is one of our best candidates for the resting state.

An even lower-energy complex would be obtained by dissociating the phosphine from complex **9** and associating another morpholine ligand to form complex **12**. The energy differences are small ( $78$  or  $82 \text{ kJ mol}^{-1}$  does not correspond to a significant difference in the computed barrier), but the observation raises the question of whether the phosphine ligand is needed for the reaction. However, a reductive elimination TS in which the phosphine has been replaced with an amine ligand has a significantly higher barrier, as the forming Pd(0) is no longer stabilized by back-donation.

**Organic Base in a Nonpolar Solvent.** Attempting to utilize DBU as a base in the reaction gives a drastically different result. The oxidative addition product with coordinated amine, complex **6**, is now among the most stable structures in the manifold. Attempts to introduce DBU as a hydrogen bond acceptor lead to a vdW complex only marginally more stable than **6**. Forcing a deprotonation and dissociation of bromide yields the necessary complex **5**, but now at a prohibitive cost of  $>200 \text{ kJ mol}^{-1}$ , giving a calculated barrier of almost  $300 \text{ kJ mol}^{-1}$ . Thus, it is clear that DBU will be incompetent as a base in a nonpolar solvent. This is not unexpected; nonpolar solvents obviously resist the formation of charge inherent in a proton transfer between neutral complexes. The only way we have been able to find a reasonable deprotonation using DBU in benzene has been to first liberate the bromide to generate a cationic Pd complex. As already shown (Figure 4), this process in itself carries a penalty of almost  $200 \text{ kJ mol}^{-1}$  in benzene. We note that this penalty is in part due to the strong bond between palladium and bromide; it has been shown previously that DBU can function as a base in arylation of anilines at high temperatures and under microwave irradiation with the more easily dissociated leaving group nonaflate.<sup>19</sup>

We note that none of the species in Figure 6 include a coordinated base. Thus, it is possible to calculate the barrier

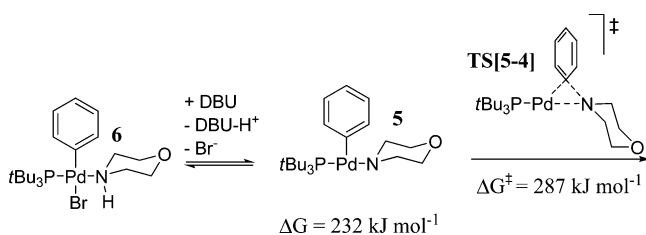


**Figure 6.** Selected structures from the Pd(II) manifold in benzene using DBU as a base.

change for other noncoordinating bases just by calculating the difference in energy between neutral and protonated forms of the base. Doing this for the very strong organic base P1 (*vide infra*), that is, replacing the energies for DBU and DBU- $\text{H}^+$  in the barrier calculation with the energies for P1 and P1- $\text{H}^+$ , we find that the barrier is reduced from the value of  $287 \text{ kJ mol}^{-1}$  we saw with DBU but is still prohibitively high ( $245 \text{ kJ mol}^{-1}$ ).

**Alkoxide Base in a Polar Aprotic Solvent.** We have chosen DMF as a typical polar aprotic solvent. The important

intermediates for the amine coordination, deprotonation, and reductive elimination are shown in Figure 7. As for the corresponding reactions in benzene, the deprotonation and ligand association equilibria have negligible barriers. The same intermediates are still present, but their relative energies have shifted substantially compared to the situation in benzene. In general, charge separation is much easier, the gain from stabilizing negative charges is less significant, and hydrogen bonds have lost most of their importance. Starting again from the direct oxidative addition product **2**, coordination of amine to give **6** is still facile. From intermediate **6**, we can still form a hydrogen bond to the base, but the process is now slightly endergonic. Proton shift and loss of bromide give neutral complex **8**. Loss of hydrogen-bonded *t*-BuOH gives **5** at a cost of only  $1 \text{ kJ mol}^{-1}$ . As before, **5** undergoes reductive elimination with a moderate barrier.

A distinct difference from benzene is that direct dissociation of bromide from **6** to yield cationic complex **7** is now a facile process. Complex **7** can associate the base to yield **9**. Complex **9** can also be formed directly from **2** by association of the base to yield anionic complex **10**, followed by facile dissociation of bromide to yield **11**. This species, despite being T-shaped and having an open coordination site, actually has a free energy lower than that of amine-coordinated species **9** and is now the resting state in the catalytic cycle.

Similar to the situation in benzene, off-cycle diamine complex **12**, without the coordinating phosphine ligand, is a low-energy species. At a high amine concentration, **12** could be present at a significant concentration. We have not found any species more than  $75 \text{ kJ mol}^{-1}$  below the reductive elimination transition state, TS[5–4], indicating that the reaction should be fast in DMF.

**Organic Base in a Polar Solvent.** Employing DBU in DMF gave results that were substantially more interesting than those in benzene. As was indicated in Figure 7, cationic complex **7** is energetically accessible in DMF. A neutral base would therefore be able to operate with a constant charge, opening a new, plausible pathway for the reaction.

Even in DMF, DBU is a substantially weaker base than *t*-BuOK. The base strength is reflected in the diagram as the energy difference between complexes **7** (where the energy includes the free base) and **5** (where the energy of the protonated base is included). We have chosen to retain TS[5–4] as the reference point at  $0 \text{ kJ mol}^{-1}$ , meaning that the energies of complex **7** and all preceding points that also include the free base implicitly will experience a downward shift compared to Figure 7. The resulting free energy profile is depicted in Figure 8.

Complex **2** can again coordinate either the amine or the base. The neutral amine coordination complex **6** does not react easily with the base; no hydrogen-bonded complex could be located with DBU. However, as also shown in Figure 7, bromide dissociation is facile. The resulting complex **7** can react with DBU to give coordination complex **13** or hydrogen-bonded complex **14**. Under these conditions, complex **13** is the resting state of the reaction. It is also possible to reach complex **13** by associating DBU directly to **2**, followed by dissociation of the bromide and association of the amine (not shown). This process is also facile but does not lead to any species lower in energy than **13** and thus does not change the reaction behavior.

From complex **14**, the proton transfers to DBU in an endergonic process, yielding **5** via hydrogen-bonded complex **15**. The overall barrier from resting state **13** to reductive

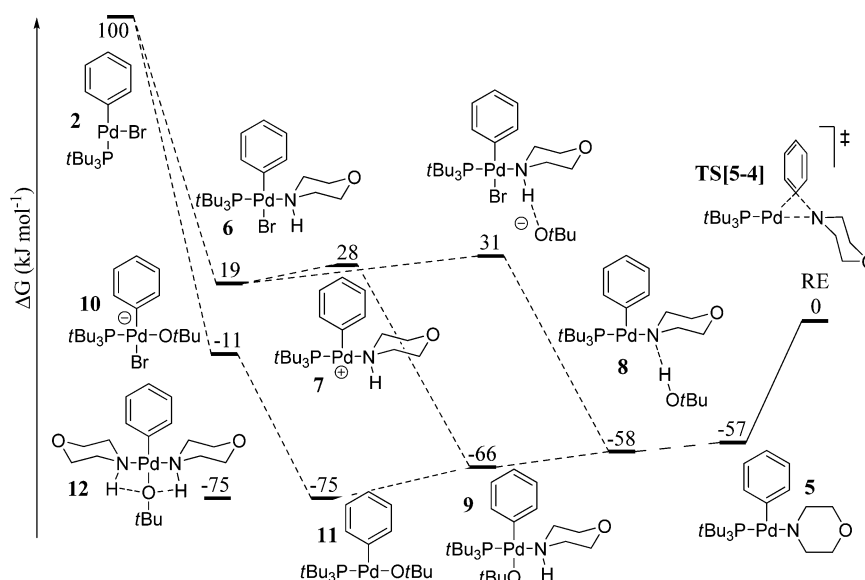


Figure 7. Selected free energies in DMF with  $t\text{-BuO}^-$  as the base.

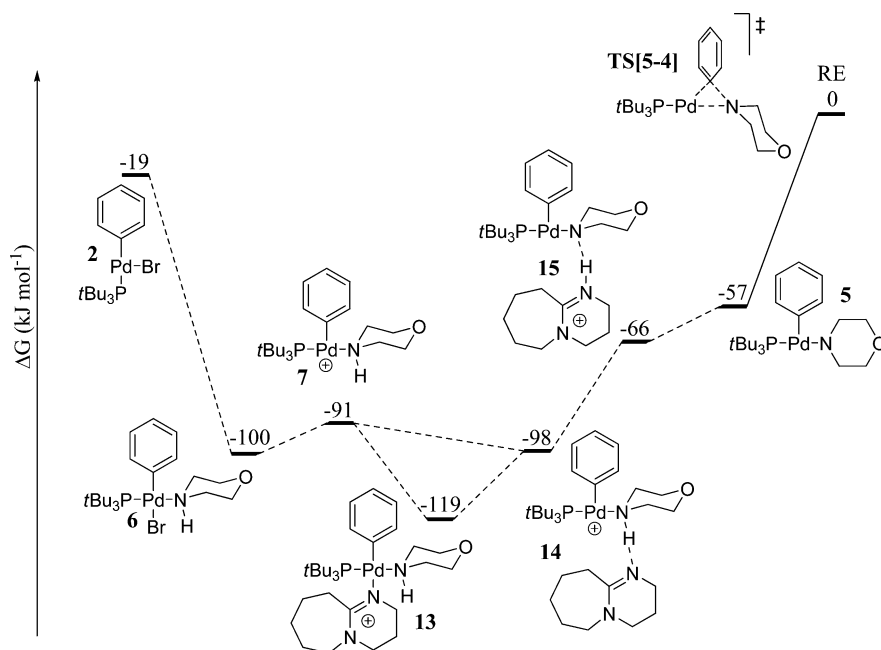


Figure 8. Free energies of important intermediates when using DBU as the base in DMF.

elimination  $\text{TS}[5-4]$  is  $119 \text{ kJ mol}^{-1}$ . This might be a feasible barrier at high temperatures, but it is dangerous to draw conclusions from absolute energies, in particular when the comparison includes a change in overall charge. It is safer to compare to the alkoxide reaction, which has a barrier of only  $75 \text{ kJ mol}^{-1}$  in DMF (Figure 7). An energy difference of more than  $40 \text{ kJ mol}^{-1}$  corresponds to a reaction that should be at least 7 orders of magnitude slower with DBU than with  $t\text{-BuOK}$  at ambient temperature, with a slightly smaller difference at higher temperature. This indicates that DBU will be an inferior base also in DMF, but it might be competent at strongly elevated temperatures with less coordinating leaving groups, as has been observed previously.<sup>19</sup>

How about other organic bases? DBU is far from the strongest of the available neutral bases. However, the resting state incorporates the base, and it is reasonable to assume that

as the base becomes stronger, complex 13 will become more stable. For the base to be competent in the reaction, the basicity must be increased while at the same time complex 13 must be destabilized, possibly by steric effects. However, the crowding around the base must not be significant enough to interfere with formation of hydrogen-bonded complex 14. The latter consideration would exclude bases like proton sponge.

**BINAP Ligand.** Studying the reaction path with the BINAP ligand is computationally demanding. The ligand is substantially larger than  $t\text{-Bu}_3\text{P}$ , with a resulting increase in computation time for each structure. The backbone is rigid, but the four pendant phenyl groups are flexible, necessitating calculations of several conformers of each structure. Finally, small bidentate ligands generally fail in the title reaction, indicating that BINAP may switch to a monodentate binding mode at some points along the reaction path. Thus, we have

limited ourselves to searching for low-energy complexes that may inhibit the reaction and finding feasible, but not necessarily the best, paths from the oxidative addition to the reductive elimination. Our findings are summarized in Figure 9. To

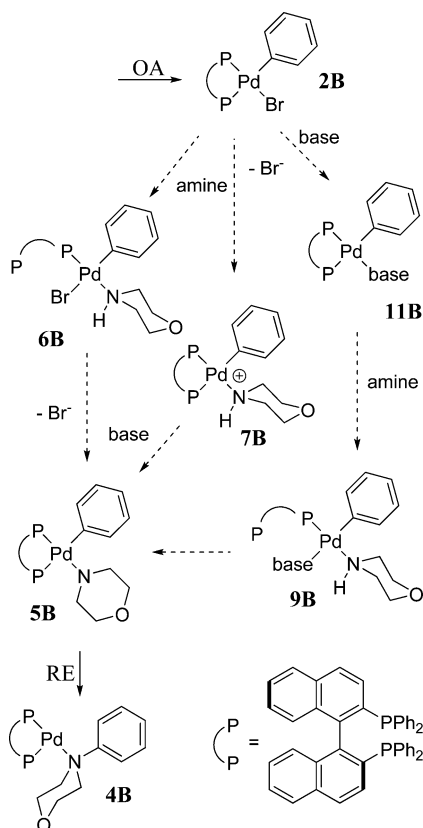


Figure 9. Mechanistic possibilities with a BINAP ligand.

simplify the comparison, names of structures are derived from the corresponding complexes in Figure 4 by the addition of a B. The energies for all intermediates with the two model solvents and bases are listed in Table 1.

Table 1. Energies of BINAP Intermediates (Figure 9) Relative to the Reductive Elimination TS (kilojoules per mole)

intermediate	benzene		DMF	
	<i>t</i> -BuO <sup>−</sup>	DBU	<i>t</i> -BuO <sup>−</sup>	DBU
2B	44	−262	28	−88
5B	−63	−63	−65	−65
6B	49	−257	57	−59
7B	149	−157	−8	−125
9B	−62	−137	−45	−86
11B	−79	−167	−75	−123
RE TS	0	0	0	0
4B	−145	−145	−142	−142

Reductive elimination, ligand exchange in Pd(0) complexes, and oxidative addition are all feasible processes with bidentate ligands. None of these processes incur a high energy penalty. However, the oxidative addition product 2B is now a coordinatively saturated square planar complex, which cannot directly associate with an additional ligand. Mechanistic possibilities include associative displacement through a trigonal

bipyramidal transition state or dissociation of the phosphine *trans* to the aryl group to liberate a coordination site. We have found the second possibility to be energetically feasible in both solvents, which is all that is needed at this point. We cannot exclude a direct associative displacement mechanism, but the reaction behavior will not change even if more facile interconversions between prereductive elimination complexes can be found, as long as we have a feasible path from 2B to the resting state, and from there to 5B. With a dissociated pendant arm, the complexes can undergo processes analogous to those depicted in Figure 4. Association of amine is now a slightly endergonic process that yields 6B from 2B. Dissociation of bromide to yield 7B is still not energetically feasible in benzene. Replacement of the bromide in 2B with alkoxide gives the resting state 11B. The energy cost for amine association with liberation of one phosphine to reach 9B is only 17 kJ mol<sup>−1</sup>. Proton transfer and elimination of *t*-BuOH give 5B. Subsequent reductive elimination has an overall barrier of only 79 kJ mol<sup>−1</sup> from 11B. It is possible to envisage a simultaneous amine coordination and deprotonation from 11B directly to 5B via a trigonal bipyramidal transition state; however, this can occur only if the direct process has a low barrier compared to the route via 9B, and even if it does exist, it will be kinetically indistinguishable from the stepwise path with a liberated arm, because the two processes share the same resting state and rate-limiting transition state.

In DMF, the bromide can dissociate before reaction with the base, giving direct access to cationic amine complex 7B. However, base complex 11B is still strongly preferred. The overall barrier is slightly lower in DMF than in benzene, only 75 kJ mol<sup>−1</sup>, but this small energy difference is probably not significant in view of the approximations that go into the continuum solvation energies.

DBU is still incompetent in both solvents, for reasons similar to those with the monodentate ligand. Formation of the protonated DBU is too costly in nonpolar solvent, and the complex with amine, 7B, is too stable to allow facile reductive elimination in DMF.

To support our experimental study (*vide infra*), we also calculated the structures in Table 1 with *N*-methylpiperazine instead of morpholine as the amine component. The results, available as Supporting Information, agree closely with the values in Table 1. Using *tert*-butoxide as a base, the overall barriers have increased by only 4–5 kJ mol<sup>−1</sup>, and the barriers using DBU are still prohibitively high, in both solvents.

**Experimental Testing.** For the experimental testing, we set up a system closely reminiscent of the computational model, but slightly more hindered on the aryl electrophile, to better model some pharmaceutically relevant electrophiles. We also changed the amine, morpholine, to the electronically very similar *N*-methylpiperazine (Figure 10). For our standard reaction, we used a palladium acetate/BINAP system, which has previously been demonstrated to be robust in kiloscale processes in the pharmaceutical industry.<sup>28</sup> Most reactions were

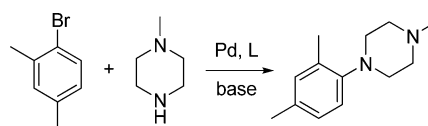
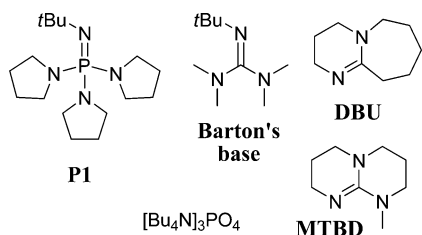


Figure 10. Experimental test system.

conducted with toluene as a solvent at 110 °C, but a few tests were performed in DMF at the same temperature.

The test system was assessed comparing two commonly used *tert*-butoxide bases with some of the stronger organic bases that are commercially available. The organic bases that were assessed are summarized in Figure 11.



**Figure 11.** Strong organic bases assessed via the Buchwald–Hartwig reaction.

In line with the computational study, the strong alkoxide bases give excellent conversions in both polar and nonpolar solvents (Table 2); however, the organic bases, even the very strong base P1, struggle to give any conversion.

**Table 2.** Experimental Test Systems, Using Bases Shown in Figure 11<sup>a</sup>

	base	solvent	conversion (%) <sup>b</sup>
1	NaO <i>t</i> -Bu	PhMe	>99
2	KO <i>t</i> -Bu	PhMe	38
3	DBU	PhMe	<1
4	KO <i>t</i> -Bu	DMF	>99
5	DBU	DMF	<2
6	P1	PhMe	<1
7	Barton's base	PhMe	<3
8	$[\text{NBu}_4]\text{PO}_4$	PhMe	<3
9	MTBD	PhMe	<3
10 <sup>c</sup>	NaO <i>t</i> -Bu	PhMe	>99

<sup>a</sup>Reactions conducted on a 1.0 mmol scale with 0.5 mol % Pd(OAc)<sub>2</sub>, 1.0 mol % BINAP, 2 equiv of NMP, and 1.4 equiv of base in 5 mL of solvent. Pd(OAc)<sub>2</sub> and BINAP were mixed at 40 °C prior to addition of other reagents. The reaction temperature was 110 °C. <sup>b</sup>Conversion reported at a 1 h reaction time and calculated by HPLC against an internal standard (*m*-terphenyl). <sup>c</sup>Pd(*t*-Bu<sub>3</sub>P)<sub>2</sub> used as a catalyst.

These results confirm the calculated results that organic bases, regardless of strength, give either disfavored transition states in nonpolar solvents or overly stable resting states in polar solvents, making them unable to effectively promote the catalytic reaction.

## CONCLUSION

Several conditions for the Pd-catalyzed arylation of morpholine have been screened computationally. For the well-established reaction using *t*-BuO<sup>−</sup> together with a hindered alkyl phosphine in a nonpolar solvent, our results agree closely with those of the preceding study of McMullin et al. The preferred path changes in polar solvent, but the major features of the reaction path remain similar. With the model organic base DBU, the reaction barrier was predicted to be prohibitively large in nonpolar solvent, mainly because of the penalty inherent in generating charge separation in the nonpolar environment. The barrier was predicted to be lower in polar solvent, but still not competitive with alkoxide bases, in part because of the overly high stability

of the resulting complex between palladium and the base. In general, a base complex seems to be either the resting state or very close in energy to the resting state when employing monodentate phosphines.

We have also located feasible pathways using a model bidentate, experimentally competent ligand, BINAP. We have shown that an energetically accessible pathway can be found if one phosphine is dissociated after the oxidative addition to allow ligand exchange and formation of the critical Pd–amide intermediate. However, we have not been able to exclude other possible pathways for this system.

Experimental testing verified the major conclusions of the computational study. The alkoxide base is competent with all tested ligands and solvents, whereas all neutral organic bases were completely unreactive under all conditions tested.

## EXPERIMENTAL SECTION

**1-(2,4-Dimethylphenyl)-4-methylpiperazine.** A Radley's carousel tube was evacuated and backfilled with nitrogen three times, before being charged with palladium acetate (11.2 mg, 0.05 mmol, 5 mol %), *rac*-2,2'-bis(diphenylphosphino)-1,1'-binaphthyl (62.3 mg, 0.1 mmol, 10 mol %), and *m*-terphenyl (20 mg, IS). Solvent (toluene or DMF, 5 mL) was then added and the reaction mixture heated to 40 °C. Once the mixture was at temperature, *N*-methylpiperazine (222 μL, 2.0 mmol, 200 mol %) was added and the reaction mixture stirred for 10 min. To this were then added 1-bromo-2,4-dimethylbenzene (136 μL, 1.0 mmol, 100 mol %) and base (see Table 2; 1.4 mmol, 140 mol %) and the reaction mixture heated to 110 °C. Reaction sampled after 1 h and conversion was calculated by HPLC against the internal standard: <sup>1</sup>H NMR (500 MHz, CDCl<sub>3</sub>) δ<sub>H</sub> 7.00–6.93 (m, 3 H, 2 × Ar-H), 2.91 (t, *J* = 4.75 Hz, 4 H, 2 × CH<sub>2</sub>), 2.57 (br s, 4 H, 2 × CH<sub>2</sub>), 2.35 (s, 3 H, CH<sub>3</sub>), 2.27 (s, 6 H, 2 × Ar-CH<sub>3</sub>); HRMS found (API+)(M + H)<sup>+</sup> 205.170, C<sub>13</sub>H<sub>21</sub>N<sub>2</sub> requires M + H 205.1699. HPLC conditions were as follows: Waters Acquity BEH-Phenyl 1.7 μm, 4.8 mm × 3.0 mm column, 5% MeCN in water, gradient to 95% MeCN over 7.5 min, held at 95% MeCN for 0.5 min, 2 mL/min, 40 °C, 232 nm, 0.03% TFA. The retention times were 4.4 min for 1-(2,4-dimethylphenyl)-4-methylpiperazine and 5.3 min for *m*-terphenyl.

**Computational Details.** All structures were determined using Becke's three-parameter hybrid functional<sup>29</sup> (B3LYP)<sup>30</sup> together with the LACVP\* basis set<sup>31</sup> as implemented in Jaguar.<sup>32</sup> All minima and transition state structures were fully optimized in the gas phase and characterized by inspection of the normal modes calculated from the analytic Hessian. An empirical term for long-range dispersion was included using DFT-D3 v1.3 by Grimme.<sup>33</sup> The thermodynamic contributions to the free energy were calculated using a temperature of 383 K, with pressures selected to reproduce the density of each solvent under an ideal gas approximation,<sup>34</sup> 361 atm for benzene and 417 atm for DMF.

The solution free energy was calculated at the final geometries using the PBF method<sup>35</sup> in Jaguar, with parameters describing benzene [dielectric constant (ε) of 2.284 and probe radius of 2.600 Å] or DMF (ε of 36.7 and probe radius of 2.490 Å). Final free energies were calculated by adding the thermodynamic and dispersion contributions to the calculated energies in solvent.

Gas phase and solvent energies using M06<sup>36</sup> with the LACVP\* basis set<sup>31</sup> were determined for the geometries of TS[5–4] and the resting states 9, 11, and 13. These energies are listed in the Supporting Information.

## ASSOCIATED CONTENT

### Supporting Information

Cartesian coordinates and energies of all calculated structures. This material is available free of charge via the Internet at <http://pubs.acs.org>.



## ■ AUTHOR INFORMATION

## Corresponding Author

\*E-mail: per-ola.norrby@astrazeneca.com.

## Notes

The authors declare no competing financial interest.

## ■ ACKNOWLEDGMENTS

The research leading to these results has received funding from the European Community's Seventh Framework Programme (FP7/2007-2013) for SYNFLOW under Grant N° NMP2-LA-2010-246461.

## ■ ADDITIONAL NOTE

<sup>a</sup>When the use of alkoxide base is being modeled, the reported energies always include the energy of an anion, that is, free alkoxide, anionic Pd complex, or free bromide.

## ■ REFERENCES

- (1) (a) Hartwig, J. F. *Acc. Chem. Res.* **1998**, *31*, 858–860. (b) Hartwig, J. F. *Nature* **2008**, *455*, 314–322. (c) Surry, D. S.; Buchwald, S. L. *Chem. Sci.* **2011**, *2*, 27–50. (d) Guram, A. S.; Rennels, R. A.; Buchwald, S. L. *Angew. Chem., Int. Ed.* **1995**, *34*, 1348–1350. (e) Louie, J.; Hartwig, J. F. *Tetrahedron Lett.* **1995**, *36*, 3609–3612.
- (2) (a) Dugger, R. W.; Ragan, J. A.; Ripin, D. H. B. *Org. Process Res. Dev.* **2005**, *9*, 253–258. (b) Schlummer, B.; Scholz, U. *Adv. Synth. Catal.* **2004**, *346*, 1599–1626.
- (3) (a) Hamann, B. C.; Hartwig, J. F. *J. Am. Chem. Soc.* **1998**, *120*, 3694–3703. (b) Hartwig, J. F.; Richards, S.; Barañano, D.; Paul, F. J. *Am. Chem. Soc.* **1996**, *118*, 3626–3633. (c) Shekhar, S.; Hartwig, J. F. *Organometallics* **2007**, *26*, 340–351.
- (4) Hoi, K. H.; Çalimsiz, S.; Froese, R. D. J.; Hopkinson, A. C.; Organ, M. G. *Chem.—Eur. J.* **2011**, *17*, 3086–3090.
- (5) Hoi, K. H.; Calimsiz, S.; Froese, R. D. J.; Hopkinson, A. C.; Organ, M. G. *Chem.—Eur. J.* **2012**, *18*, 145–151.
- (6) McMullin, C. L.; Bastian, R.; Besora, M.; Orpen, G. A.; Harvey, J. N.; Fey, N. J. *Mol. Catal. A: Chem.* **2010**, *324*, 48–55.
- (7) (a) Barder, T. E.; Biscoe, M. R.; Buchwald, S. L. *Organometallics* **2007**, *26*, 2183–2192. (b) Barder, T. E.; Buchwald, S. L. *J. Am. Chem. Soc.* **2007**, *129*, 12003–12010. (c) Cundari, T. R.; Deng, J. J. *Phys. Org. Chem.* **2005**, *18*, 417–425. (d) Green, J. C.; Herbert, B. J.; Lonsdale, R. J. *Organomet. Chem.* **2005**, *690*, 6054–6067.
- (8) Hartwig, J. *Organotransition Metal Chemistry: From Bonding to Catalysis*; University Science Books: Sausalito, CA, 2010.
- (9) Buchwald, S. L.; Surry, D. S. *Angew. Chem., Int. Ed.* **2008**, *47*, 6338–6361.
- (10) (a) Wolfe, J. P.; Buchwald, S. L. *J. Org. Chem.* **1997**, *62*, 1264–1267. (b) Meadows, R. E.; Woodward, S. *Tetrahedron* **2008**, *64*, 1218–1224.
- (11) (a) Kocovsky, P.; Vyskocil, S.; Cisarova, I.; Srjbal, J.; Tislerova, I.; Smrcina, M.; Lloyd-Jones, G. C.; Stephen, S. C.; Butts, C. P.; Murray, M.; Langer, V. *J. Am. Chem. Soc.* **1999**, *121*, 7714–7715. (b) Yin, J.; Rainka, M. P.; Zhang, X.-X.; Buchwald, S. L. *J. Am. Chem. Soc.* **2002**, *124*, 1162–1163.
- (12) Bäcktorp, C.; Norrby, P.-O. *Dalton Trans.* **2011**, *40*, 11308–11314.
- (13) Schulte, J. P., II; Tweedie, S. R. *Synlett* **2007**, *15*, 2331–2336.
- (14) Naber, J. R.; Buchwald, S. L. *Angew. Chem., Int. Ed.* **2010**, *49*, 9469–9474.
- (15) Hopkin, M. D.; Baxendale, I. R.; Ley, S. V. *Chem. Commun.* **2010**, *46*, 2450–2452.
- (16) Nishiyama, M.; Yamamoto, T.; Koie, Y. *Tetrahedron Lett.* **1998**, *39*, 617–620.
- (17) Hartwig, J. F.; Kawatsura, M.; Hauck, S. I.; Shaughnessy, K. H.; Alcazar-Roman, L. M. *J. Org. Chem.* **1999**, *64*, 5575–5580.
- (18) The conformational search problem would necessitate the use of a much faster yet accurate modeling method. Such a method was not available in our case. However, evaluations of several thousand structures can be done if a suitable molecular mechanics method can be utilized. For an example of a modeling study including alkali counterion effects, see: Butts, C.; Filali, E.; Guy Lloyd-Jones, G.; Norrby, P.-O.; Sale, D.; Schramm, Y. *J. Am. Chem. Soc.* **2009**, *131*, 9945–9957.
- (19) Tundel, R. E.; Anderson, K. W.; Buchwald, S. L. *J. Org. Chem.* **2006**, *71*, 430–433.
- (20) Clot, E.; Norrby, P.-O. In *Innovative Catalysis in Organic Synthesis: Oxidation, Hydrogenation, and C-X Bond Forming Reactions*; Andersson, P., Ed.; Wiley-VCH: Weinheim, Germany, 2012; pp 167–191.
- (21) Kozuch, S.; Shaik, S. *Acc. Chem. Res.* **2011**, *44*, 101–110.
- (22) McMullin, C. L.; Jover, J.; Harvey, J. N.; Fey, N. *Dalton Trans.* **2010**, *39*, 10833–10836.
- (23) Ahlquist, M.; Norrby, P.-O. *Organometallics* **2007**, *26*, 550–553.
- (24) (a) Fairlamb, I. J. S.; Kapdi, A. R.; Lee, A. F. *Org. Lett.* **2004**, *6*, 4435–4438. (b) Fairlamb, I. J. S.; Kapdi, A. R.; Lee, A. F.; McGlacken, G. P.; Weissburger, F.; de Vries, A. H. M.; Schmieder-van de Vondervoort, L. *Chem.—Eur. J.* **2006**, *12*, 8750–8761. (c) Firmansjah, L.; Fu, G. C. *J. Am. Chem. Soc.* **2007**, *129*, 11340–11341.
- (25) Ahlquist, M. S. G.; Norrby, P.-O. *Angew. Chem., Int. Ed.* **2011**, *50*, 11794–11797.
- (26) Cramer, C. J. *Essentials of Computational Chemistry: Theories and Models*, 2nd ed.; Wiley: Chichester, U.K., 2004.
- (27) Nilsson Lill, S. O.; Ryberg, P.; Rein, T.; Bennström, E.; Norrby, P.-O. *Chem.—Eur. J.* **2012**, *18*, 1640–1649.
- (28) (a) Federsel, H.-J.; Hedberg, M.; Qvarnström, F. R.; Tian, W. *Org. Process Res. Dev.* **2008**, *12*, S12–S21. (b) Federsel, H.-J.; Hedberg, M.; Qvarnström, F. R.; Sjögren, M. P. T.; Tian, W. *Acc. Chem. Res.* **2007**, *40*, 1377–1384.
- (29) Becke, A. D. *J. Chem. Phys.* **1993**, *98*, 5648–5652.
- (30) Stephens, P. J.; Devlin, F. J.; Chabalowski, C. F.; Frisch, M. J. *J. Phys. Chem.* **1994**, *98*, 11623–11627.
- (31) The lacvp\* basis set uses 6-31G\* for light elements, whereas lacvp3p\* uses 6-311G\*\*. Both basis sets use the Hay-Wadt ECP with the accompanying basis set for Pd: Hay, P. J.; Wadt, W. R. *J. Chem. Phys.* **1985**, *82*, 299–310.
- (32) *Jaguar*, versions 7.7–8.4; Schrodinger, LLC, New York. For the most recent version, see [www.schrodinger.com](http://www.schrodinger.com).
- (33) Grimme, S.; Antony, J.; Ehrlich, S.; Krieg, J. *J. Chem. Phys.* **2010**, *132*, 154104.
- (34) Martin, R. L.; Hay, P. J.; Pratt, L. R. *J. Phys. Chem. A* **1998**, *102*, 3565–3573.
- (35) Marten, B.; Kim, K.; Cortis, C.; Friesner, R. A.; Murphy, R. B.; Ringnalda, M. N.; Sitkoff, D.; Honig, B. *J. Phys. Chem.* **1996**, *100*, 11775–11788.
- (36) Zhao, Y.; Truhlar, D. G. *Theor. Chem. Acc.* **2008**, *120*, 215–241.